# Improving compactness for active noise control of a small axial cooling fan

Brian B. Monson,[a] Scott D. Sommerfeldt[b] and Kent L. Gee[c]

(Received 2006 September 12; revised 2007 May 07; accepted 2007 May 10)

**An active noise control (ANC) system was previously developed by Gee and Sommerfeldt for the reduction of tonal noise radiated by small axial cooling fans, such as those found in desktop computers. That system had a 125 × 125-mm$^2$ footprint, composed of four small loudspeakers surrounding an 80 × 80-mm$^2$ axial cooling fan in a mock computer casing. A smaller system is described in this paper that has a footprint of 80 × 80 mm$^2$, which is the space allotted for the 80 × 80-mm$^2$ standard sized fan. Compared with the previous system, the current system employs a smaller fan running at a higher speed and smaller control speakers. It is demonstrated that the higher output noise levels and higher frequency tones produced by the smaller fan can be reduced by the current ANC system, such that the global control achieved by the smaller system is comparable or better than that achieved by the previous system for the targeted frequencies. It is also shown that control at the second and third harmonics of the blade passage frequency approach theoretical limits.**


Primary subject classification: 38.2; Secondary subject classification: 11.4.1

## 1 INTRODUCTION

The active control of noise radiated by small axial cooling fans has received some recent scientific attention, particularly with regard to fans found in typical electronic office equipment (e.g., desktop computers). Noise radiated from these fans affects the workplace, the home, and the classroom. Such noise can be disturbing or distracting and cause unnecessary annoyance. While these noise levels are typically not high enough to cause hearing damage, it has been found that prolonged exposure to even low levels of office noise can be detrimental to health and well being[1].

Fan noise is characterized acoustically by discrete tones superposed on a broadband spectrum, as can be seen in Fig. 1. These tones are caused by spatially unsteady time-invariant fluid loading on the rotating fan blades. This loading may be ascribed to flow obstructions near the inlet or exhaust of the fan, such as stators or finger guards. The tones present in the fan noise spectrum are found to be both harmonically related to each other and related to the rotational speed of the fan. The first major tone, referred to as the blade passage frequency (BPF), often lies between 100 and 600 Hz for cooling fan applications. The BPF generally exhibits the highest radiation level and is calculated, in hertz, from revolutions per minute (RPM) as

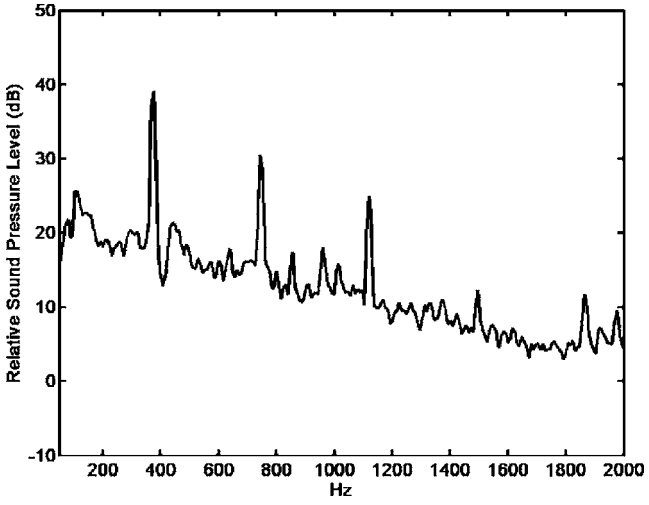


*Fig. 1—A typical power spectrum of fan noise consisting of both broadband and tonal noise.*

[a] Brigham Young University, Department of Physics and Astronomy, N283 ESC BYU, Provo, UT 84602; email: brainbmonson@byu.net.
[b] Brigham Young University, Department of Physics and Astronomy, N283 ESC BYU, Provo, UT 84602; email: scott_sommerfeldt@byu.edu.
[c] Brigham Young University, Department of Physics and Astronomy, N283 ESC BYU, Provo, UT 84602; email: kentgee@byu.edu.

$$BPF = N \times \frac{RPM}{60}, \quad (1)$$

where $N$ is the number of blades on the fan. Although both noise components mentioned are present in the spectrum of cooling fan noise, the BPF and harmonics typically dominate the overall sound pressure level and perceived noise level[2]. Tonal noise has therefore been the emphasis of most studies on fan noise reduction.

Active noise control has become an increasingly attractive solution for the reduction of fan noise because of ongoing refinements in digital signal processing technology. Notable efforts have been made to combat the axial fan noise problem in the free field with some successful results. Quinlan[3] achieved global sound power reductions of 12 dB for the BPF, and 7 dB for the second harmonic, by using a single secondary control source loudspeaker placed next to a fan in a baffle. Wu[4] showed confirming results, with a setup similar to that of Quinlan. Lauchle et al.[5] utilized the fan itself as the secondary control source by driving the fan with a shaker. This approach resulted in sound power reductions of 13 dB and 8 dB for the BPF and second harmonic, respectively. Homma et al.[6] added a duct and multi-channel control and incorporated hybrid active and passive control. Their method exhibited both tonal and broadband noise reduction, with an overall sound power reduction of 4.9 dB.

A study performed by Gee and Sommerfeldt[7] showed that multiple control sources surrounding the fan resulted in global reductions of the BPF and harmonic levels. The study reported spatially averaged squared pressure reductions of 10.1 dB, 15.3 dB, 12.8 dB, and 8.7 dB for the fundamental, second, third, and fourth harmonics, respectively. This control system was based on a multi-channel version of the filtered-x LMS algorithm developed by Sommerfeldt[8].

There are three points of particular significance in the control approach taken by Gee and Sommerfeldt that distinguish it from previous work. These are: (1) extension to multiple control sources of Quinlan's coplanar control-source/fan arrangement, (2) implementation of multi-channel adaptive control, and (3) use of microphone(s) placed in the near-field of a fan as a robust, stable method of noise control. The study further proposed that optimal locations for these error sensors exist coplanar with the fan and control actuators, such that global control may be achieved[9]. The research of Gee and Sommerfeldt is the basis for the current work.

An 80-mm fan, which has been a standard size for desktop computer cooling applications, was used by Gee and Sommerfeldt. The fan with the control system embedded, however, required an area of 125 $\times$ 125 mm$^2$. Because of industry efforts to continue to decrease the size of desktop computers, a control and fan configuration that fit within the standard 80 $\times$ 80-mm$^2$ area was desired for a more commercially viable system. The primary objective of this research was to determine if a smaller fan and control system could demonstrate similar control performance to that of the original system. It was found that a 60-mm fan and suitably sized loudspeakers could fit within the desired spatial footprint. A description of the performance of the smaller control system and a comparison of the 60-mm fan configuration to that of the 80-mm fan follow.

## 2 THEORETICAL MODEL

### 2.1 Underlying Theory

Typically, if the principle of mutual coupling can be employed in the active control of a noise source radiating into free space, the resultant control behavior is of a more global nature, and is therefore more desirable.

As two monopole sources radiating into free space are brought into near-field proximity with one another, the mutual impedance seen by each source is modified due to the presence of the other source[10,11]. The total power, $W$, radiated by both sources is determined analytically to be

$$W = \frac{k^2 \rho c}{8\pi} |\tilde{Q}_1|^2 \left[ 1 + A^2 + 2A \frac{\sin kd}{kd} \cos \gamma \right], \quad (2)$$

where

$$\frac{\tilde{Q}_2}{\tilde{Q}_1} = A e^{j\gamma}, \quad (3)$$

$k$ is the acoustic wave number, $\rho$ is the density of the medium (kg/m$^3$), $c$ is the speed of sound (m/s), and $d$ is the separation distance (m) between the two sources. The variables $\tilde{Q}_1$ and $\tilde{Q}_2$ represent the complex monopole source strengths. Minimization of Eqn. (2) by optimizing the secondary source strength, $\tilde{Q}_2$, relative to the primary source strength, $\tilde{Q}_1$, leads to the optimal control source strength,

$$\tilde{Q}_2 = -\tilde{Q}_1 \frac{\sin(kd)}{kd},$$

and the minimum power radiated by both sources,

$$W_{MIN} = \frac{k^2 \rho c}{8\pi} |\tilde{Q}_1|^2 \left[ 1 - \left( \frac{\sin kd}{kd} \right)^2 \right]. \quad (5)$$

The right-hand side of Eqn. (5) may be further rewritten to contain the expression representing the power radiated by a single monopole source ($W_{MONO}$) of

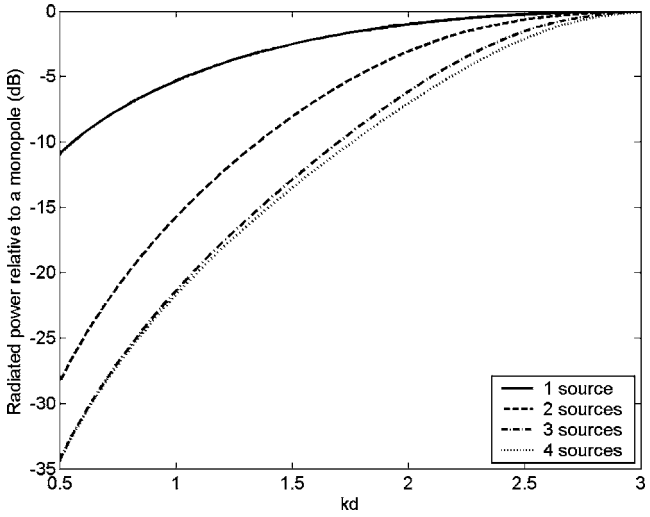


*Fig. 2—Theoretical minimum radiated power for control source arrangements of one, two, three, and four symmetrically spaced monopole secondary sources surrounding a primary monopole source. The control source(s) are coplanar with the primary source.*

strength $\tilde{Q}_1$. This allows $W_{MIN}$ to be expressed as

$$W_{MIN} = W_{MONO}\left[1 - \left(\frac{\sin kd}{kd}\right)^2\right]. \quad (6)$$

## 2.2 Control Source Configuration

The preceding theoretical discussion may also be applied to scenarios with multiple control sources. Some plausible arrangements for control sources for a practical system consist of the fan surrounded by two, three, and four symmetrically spaced control sources in a plane. Generally, an unbaffled and uncontrolled fan will radiate primarily as a dipole source. However, as shown by others[3,5], the radiation characteristics of a baffled fan approximate those of a monopole. This can also be seen later in this paper, with the measured results of the uncontrolled fan (see Figs. 8–13). If the fan is treated as a monopole, extension of the secondary source optimization technique to these systems gives the minimum radiated power for each configuration. The results of this analysis have been studied by Nelson and Elliot[10] and Gee and Sommerfeldt[9] and are shown in Fig. 2. For these results, the total radiated sound power has been calculated and then minimized. In the figure, the minimum power radiation, relative to the power radiated by a single monopole, is plotted as a function of *kd*. For these configurations, the solutions for the optimal control source strengths for two, three, and four control sources may be expressed respectively as

$$\tilde{Q}_2 = -\tilde{Q}_1 \frac{\sin(kd)}{kd}\left\{\frac{1}{1+\sin(2kd)/2kd}\right\},$$

$$\tilde{Q}_2 = -\tilde{Q}_1 \frac{\sin(kd)}{kd}\left\{\frac{1}{1+2\sin(\sqrt{3kd})/\sqrt{3kd}}\right\}, \quad (8)$$

and

$$\tilde{Q}_2 = -\tilde{Q}_1 \frac{\sin(kd)}{kd} \times\left\{\frac{1}{1+\sin(2kd)/2kd+2\sin(\sqrt{2kd})/\sqrt{2kd}}\right\}. \quad (9)$$

For the 60-mm fan configuration, the separation distance was 0.045 m, measured from the center of the fan to the center of the control loudspeaker. The BPF was 600 Hz, resulting in *kd* values of approximately 0.5, 1.0, and 1.5 for the BPF and its second and third harmonics, respectively. Although the analysis shown was developed for the free-field case, the relative strengths of the noise source and control sources for the current application, as well as the minimum power radiation plot, are identical to the free-field case, in that the presence of a baffle simply scales all source strengths by a factor of two.

From Fig. 2 it can be seen that as *kd* becomes very small, radiated power is greatly decreased, whereas *kd* approaching $\pi$ leads to very little or no reduction of radiated power. It is also important to note that as *kd* becomes small there also appears to be very little difference in the curves depicting the attenuation for three and four control sources. In other words, increasing the number of coplanar secondary sources to greater than four tends to bring little gain in sound power attenuation for all values of *kd*[9]. Both the three- and four-source configurations were implemented as a part of this research, but the primary focus has been the four-source configuration because of the ease in fitting the system in an $80 \times 80$-mm$^2$ area.

## 2.3 Error Sensor Location

Error sensors are needed in order to implement the filtered-x LMS control algorithm. Error sensor microphone placement may be optimized by finding the regions of greatest pressure attenuation when the global sound power radiation is minimized[11]. Based on Gee and Sommerfeldt's method[9], an analysis of such regions coplanar with a simple source and four symmetrically spaced control sources can be seen in Figs. 3 and 4. Each plot shows computational results for the controlled pressure field in decibels relative to

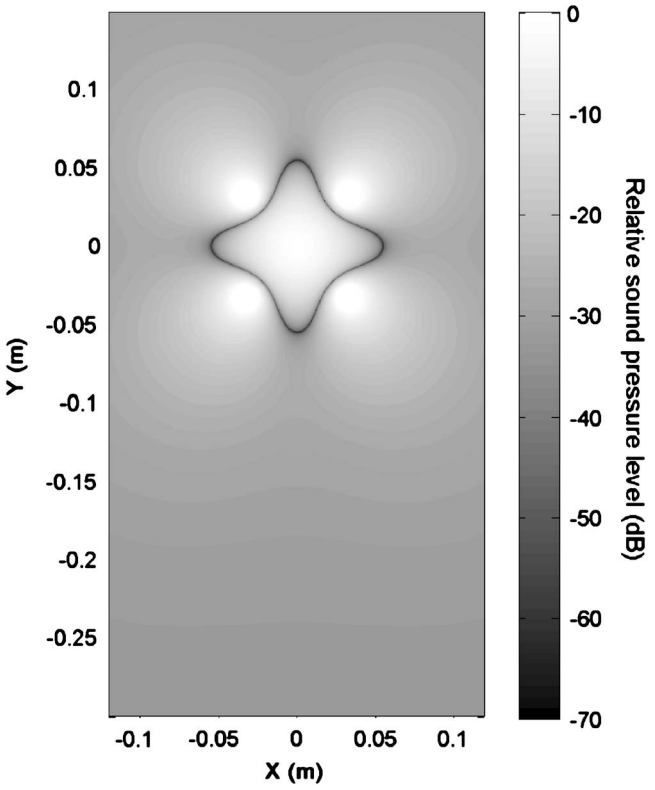


*Fig. 3—Theoretically predicted controlled acoustic pressure field of a plane containing a noise source and four control sources at* 600 Hz*, relative to the pressure field of a single monopole. The dark line indicates a pressure null demarcating optimal error sensor location on the plane.*

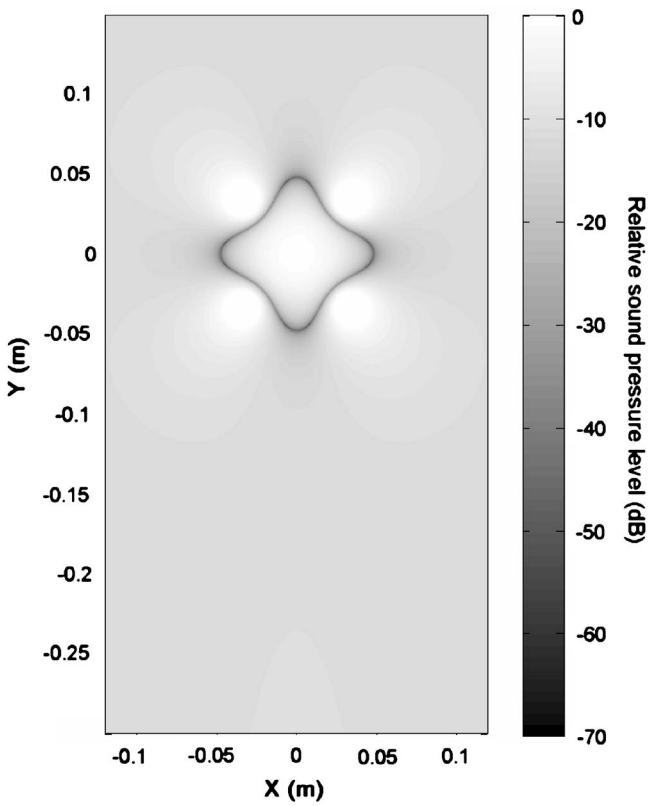


*Fig. 4—Theoretically predicted controlled acoustic pressure field of a plane containing a noise source and four control sources at* 1800 Hz*, relative to the pressure field of a single monopole.*

the pressure field of a single noise source. The dark closed contour represents a pressure null. This null shape varies slightly depending upon frequency and separation distance from the noise source to the control sources. Figure 3 shows the 600-Hz case (the BPF of the 60-mm fan) with a separation distance of 0.045 m. Figure 4 displays the attenuation of 1800 Hz (3 $\times$ BPF) with the same separation distance. The control sources are situated around the noise source and are indicated by the bright regions (corresponding to 0 dB) at 45, 135, 225, and 315 degrees.

If error sensor location is constrained to the plane of the sources, optimal locations for error sensors may be found by locating points on the plane that are common to the null contours for all frequencies of interest. This method, however, is not without its limitations in a practical application. In the case of fan noise active control, positions must be selected that are sufficiently far from the fan to achieve an acceptable signal-to-noise ratio. Placement of sensors too close to the fan causes an increase in noise due to turbulent airflow across the microphone diaphragm.

With these considerations, locations were initially chosen on the null pattern corresponding to points that lay on the source plane null contour and were common for all harmonics of interest. These points were located near each control loudspeaker. Numerous locations near the ideal locations were used for testing and those giving the best results were implemented. The implemented locations were located 4.8 cm from the center of the fan in the positive x-direction, and 1.2 cm in the positive y-direction. These coordinates were repeated for each error sensor relative to 0°, 90°, 180°, and 270° from the fan axis, as shown in Fig. 5. The locations are seen to correspond well with the predicted pressure null. Sensors placed in this arrangement gave the best control performance of all measurements taken. The results are discussed more specifically in Sec. 4.

## 3 EXPERIMENTAL SETUP

A fan housed in a mock computer casing was used for experimental testing. The aluminum casing, shown in Fig. 6, was 0.45 m in height, 0.4 m in length, and 0.25 m in width. The fans used were 80-mm and 60-mm Mechatronics DC cooling fans. The control

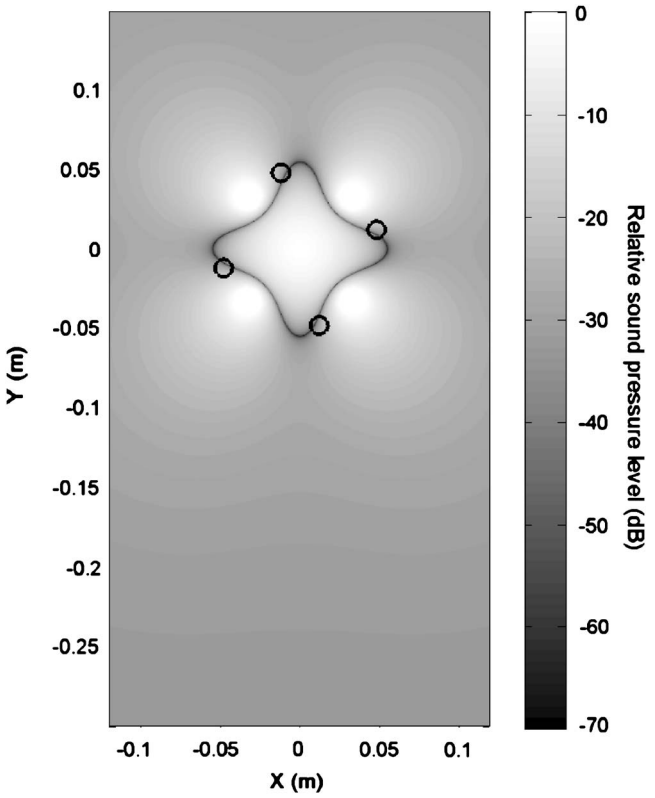


*Fig. 5—Source plane plot at* 600 Hz *showing theoretically predicted controlled field, with the markers indicating experimentally implemented error sensor locations.*

arrangement for the 80-mm fan consisted of four 29-mm Radio Shack model 273-092 loudspeakers located coplanar with and surrounding the fan. The

*Fig. 6—An aluminum mock computer casing shown under a rotating semicircular microphone boom located in the anechoic chamber on the Brigham Young University campus.*

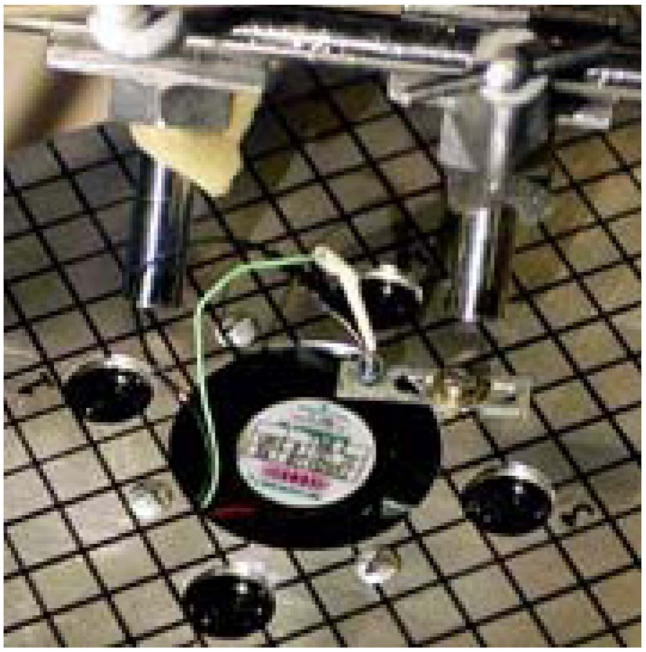

*Fig. 7—The* 60-mm *fan surrounded by four* 20-mm *miniature loudspeakers.*

60-mm control arrangement, embedded in the top wall (0.45 m × 0.25 m) of the casing, is seen in Fig. 7. The fans used were mounted in this top panel, with the center of the fan located at a position (0.15 m, 0.125 m) from the corner, as can be seen in Figs. 3 and 4. Four Regal Electronics R-20-E miniature loudspeakers, 20 mm in diameter, were selected as control actuators. The control sources were spaced symmetrically around the 60-mm fan, fitting within an 80 × 80-mm area. Miniature loudspeakers present a problem in that their low-frequency response is generally poor, and the power handling capability of the loudspeakers is usually rather limited. With typical BPFs found below 1000 Hz, it is essential for effective control that control actuators have a good response in this region. To improve the response of the loudspeakers, each was enclosed separately within the computer casing by a small PVC enclosure, with an effective volume of $13.6 \times 10^{-6}$ m$^3$. The enclosures were further optimized by the addition of two small ports, with length 2.38 mm and combined surface area $31.4 \times 10^{-6}$ m$^2$, creating a bass-reflex system. The enclosure was tuned to a resonance frequency of 600 Hz.

Located on the 60-mm fan were seven blades and three support struts. The fan was run at a constant voltage, near 10 V, giving an approximate rotational speed of 5140 RPM. An 18-mm wide 60-mm long rectangular aluminum obstruction was placed directly behind one edge of the fan to simulate possible stationary obstructions found in a computer casing. An infrared emitter/detector pair placed on either side of the fan

was used to determine the BPF and served as a reference sensor for the feed-forward adaptive control algorithm discussed previously. The reference input sensor was low-pass filtered to retain only those harmonics below 2 kHz, and amplified to provide an input level to the DSP of about ±1.5 V.

Four Larson Davis 2551 12.7-mm (1/2-in.) Type-1 microphones with Larson Davis PRM426 preamplifiers (see Fig. 7) were used as error sensors for the control system. The preamplifiers were fed to a 12-channel power supply. The error sensor signals were high-pass filtered at 500 Hz using a Krohn-Hite Model 3364 4-pole Butterworth filter to eliminate low-frequency noise from turbulent airflow. In later testing, the Larson Davis microphones were replaced by small electret microphones to verify that inexpensive microphones could be used. The results with those error sensors were found to be statistically no different than those presented here.

All measurements were taken in an anechoic chamber located on the Brigham Young University campus. Figure 6 shows a rotating semicircular boom used to measure the sound pressure level at equally spaced points away from the casing. The boom was 3.04 m in diameter, with thirteen additional Larson Davis 2551 Type-1 microphones placed at 15° increments around the boom. The boom was rotated clockwise in ten 18° increments to obtain a total of 130 data points for each global sound pressure measurement. Spectral data from the boom microphones were acquired using a VXI-based Hewlett-Packard multichannel dynamic signal analyzer with Data Physics SignalCalc® analysis software.

The filtered-x LMS algorithm was implemented using a Spectrum 96000 floating-point digital signal processing board, mounted in a computer with a 486 processor. The sampling frequency was 4 kHz for all measurements shown for the 60-mm system. The control outputs from the computer were low-pass filtered at 2 kHz to prevent aliasing effects in the digital to analog conversion process. The computer and DSP hardware were located in a control room separate from the anechoic chamber, so that all measurements and control tests were performed remotely.

## 4 EXPERIMENTAL RESULTS

For the 80-mm fan, the BPF was 370 Hz (see Fig. 1), and its first few harmonics were present in the noise spectrum. Figures 8–10 show plots of the previous reduction achieved for the first three harmonics of the 80-mm fan control system.

Gee and Sommerfeldt[7] previously used a spatially averaged squared pressure reduction to quantify global reductions. However, a more common measure for

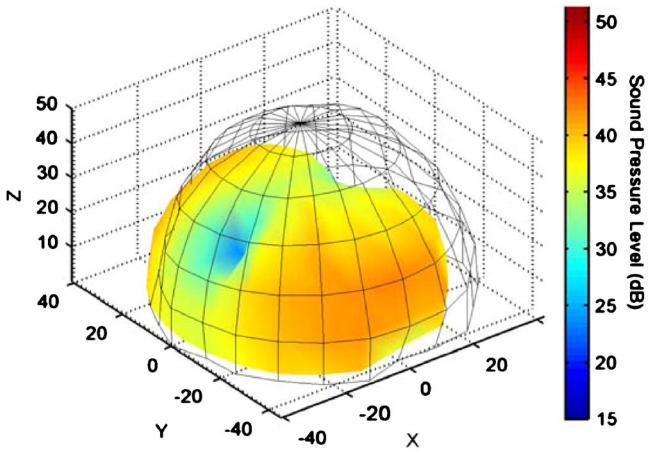


*Fig. 8—Experimentally measured far-field acoustic pressure at* 370 Hz *(BPF) for the* 80-mm *fan, without and with control. The wire mesh indicates control off, with radius indicating sound pressure level in that direction. The shaded surface indicates control on, with radius and color scale indicating sound pressure level.*

determining global attenuation is the sound power reduction (SPR). Calculation of this quantity also permits direct comparison of experimental to theoretical results. Thus, a method was used to convert the array of measured pressure values into a sound power estimate. The method used to obtain the sound power estimate followed a method similar to that described by

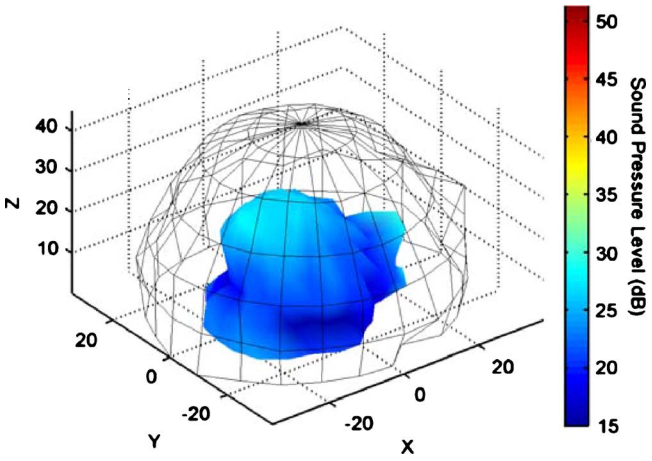


*Fig. 9—Experimentally measured far-field acoustic pressure at* 740 Hz (2 × BPF) *for the* 80-mm *fan, without and with control. The wire mesh indicates control off, with radius indicating sound pressure level in that direction. The shaded surface indicates control on, with radius and color scale indicating sound pressure level.*

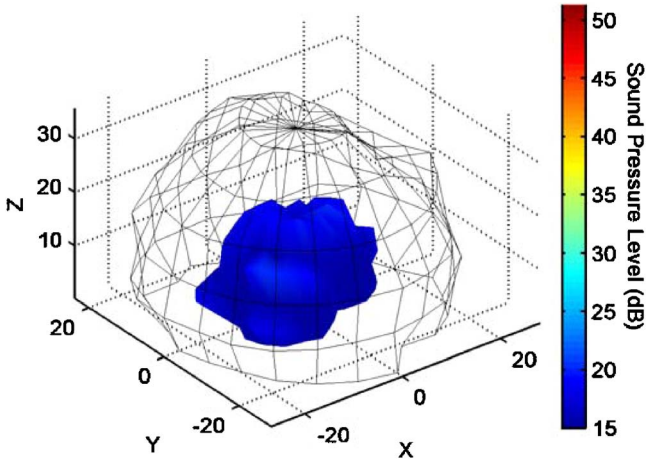


*Fig. 10—Experimentally measured far-field acoustic pressure at* 1110 Hz (3 × BPF) *for the* 80-mm *fan, without and with control. The wire mesh indicates control off, with radius indicating sound pressure level in that direction. The shaded surface indicates control on, with radius and color scale indicating sound pressure level.*

Leishman et al.[12] Sound power level over the hemisphere was calculated as

$$L_{\Pi} \approx 10 \log\left[\sum_{i=1}^{13}\sum_{n=1}^{10} A_i 10^{0.1 L_{p_{ni}}}\right], \qquad (10)$$

where $L_{Pni}$ is the sound pressure level at the $i$th microphone position and the $n$th boom rotation position of a semicircle rotated 180 degrees. The microphone positions are shown schematically in Fig. 11. An area weighting function, $A_i$, was applied to the pressure measured at the $i$th microphone position located on a semicircle of radius $r$, defined by

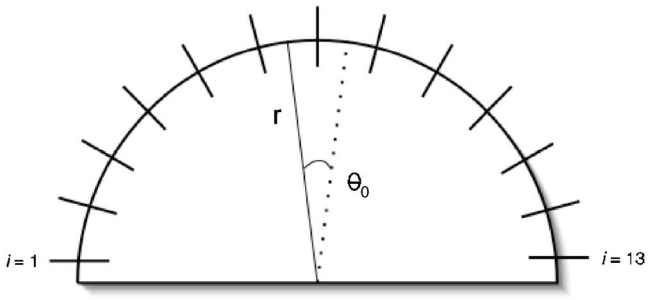


*Fig. 11—Diagram depicting microphone spacing on a semicircular microphone boom.*

$$A_i = \begin{cases} r^2\phi_0 \cos\theta_{i+1}; & i = 1 \\ r^2(\cos\theta_{i+1} - \cos\theta_i)\phi_0; & 2 \leq i \leq 6 \\ 2\pi r^2\left(1 - \cos\frac{\theta_0}{2}\right); & i = 7 \\ r^2(\cos\theta_i - \cos\theta_{i+1})\phi_0; & 8 \leq i \leq 12 \\ r^2\phi_0 \cos\theta_i; & i = 13 \end{cases}, \qquad (11)$$

with angles defined as

$$\theta_i = \theta_0(i-7) - \frac{\theta_0}{2},$$

$$\theta_0 = 15\,^\circ,$$

$$\phi_0 = 18\,^\circ. \qquad (12)$$

This area weighting is necessary since the boom microphones are configured for "equal angle" measurements (appropriate for directivity) rather than for "equal area" measurements (appropriate for sound power).

In the plots, the mesh surface represents the sound pressure level of the fan radiating without active control, and the solid surface is the radiation with control running. The plots give global sound pressure level measurements in dB re 20 $\mu$Pa, with pressure level indicated by both radius and color scale shading (for control on). It is noted that the fan and control system are raised 0.45 m above the ground, which leads to a skewing of the pressure levels toward the positive z-direction. The previously reported spatially averaged squared pressure reductions of 10.1 dB, 15.3 dB, and 12.8 dB were averaged values of several experiments evaluating the 80-mm control system performance. In this paper the best-case results will be examined and all results are based on sound power reduction (SPR). For the first three harmonics, the 80-mm control system achieved SPR of 6.7 dB, 16.5 dB, and 14.9 dB, respectively. Though not shown, the control system also attenuated the fourth harmonic by 9.6 dB.

The BPF for the 60-mm fan was 600 Hz, with the second and third harmonics at 1200 Hz and 1800 Hz. Global reduction plots of the 60-mm fan noise are shown in Figs. 12–14. The SPR, calculated as before, was found to be 14.5 dB, 16.6 dB, and 9.0 dB for the fundamental, second, and third harmonic, respectively. It is interesting to note that the mesh surfaces reveal the omni-directional behavior of the fan's BPF without control, suggesting monopole-like characteristics.

The results in Fig. 2 suggest an additional step that can be taken to improve the compactness of the control system. From Fig. 2, it appears that three symmetrically placed control sources could be used instead of four,

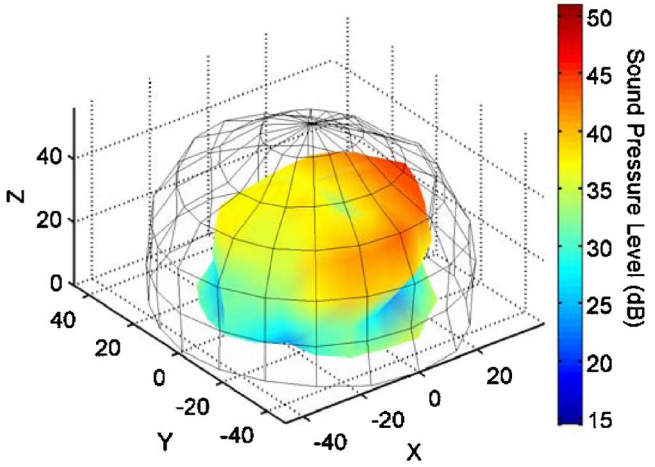


*Fig. 12—Experimentally measured far-field acoustic pressure at* 600 Hz *(BPF) for the* 60-mm *fan, without and with control. The wire mesh indicates control off, with radius indicating sound pressure level in that direction. The shaded surface indicates control on, with radius and color scale indicating sound pressure level.*

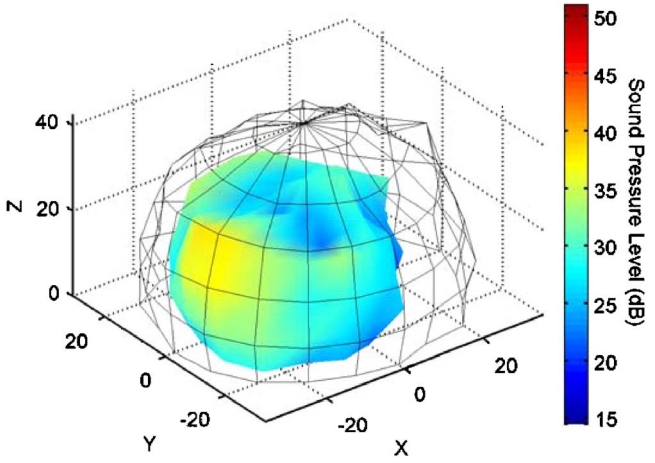


*Fig. 14—Experimentally measured far-field acoustic pressure at* 1800 Hz (3 × BPF) *for the* 60-mm *fan, without and with control. The wire mesh indicates control off, with radius indicating sound pressure level in that direction. The shaded surface indicates control on, with radius and color scale indicating sound pressure level.*

with minimal degradation in performance. From a practical perspective, this is a little more difficult with existing fans, since typical fans are manufactured with a square geometry, which means a symmetric configuration of three control sources with minimal spacing between the fan and control sources requires modification of the structure surrounding the fan. Nonetheless, a fan was modified to accommodate this configuration, in order to verify predictions. The theoretical pressure field for this configuration is shown in Fig. 15, including the implemented error sensor locations. The SPR achieved for each harmonic using the three-loudspeaker control system is shown in Table 1. As predicted by the theoretical result in Fig. 2, the global performance of the three- and four-loudspeaker systems is very similar.

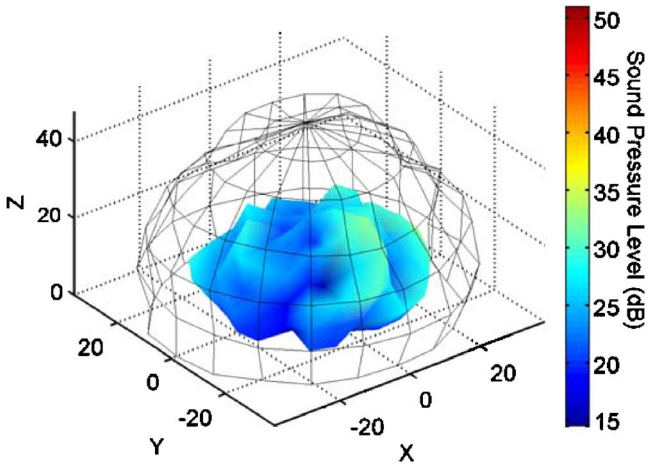


*Fig. 13—Experimentally measured far-field acoustic pressure at* 1200 Hz (2 × BPF) *for the* 60-mm *fan, without and with control. The wire mesh indicates control off, with radius indicating sound pressure level in that direction. The shaded surface indicates control on, with radius and color scale indicating sound pressure level.*

## 5 DISCUSSION

It is seen from Figs. 8–10 and 12–14 that the 80-mm system and the 60-mm system demonstrated similar control performance. Both were able to achieve global control of the first three harmonics of the BPF, though attenuation of the BPF itself was notably less than the second harmonic in both cases. Table 2 outlines the comparison of *kd* values and attenuations of the two systems versus the theoretically ideal sound power reduction predicted by Gee and Sommerfeldt[9].

### 5.1 60-mm System vs. Theory

An examination of the 60-mm system performance reveals that it did not achieve optimal control of the fan BPF. This is indicated by the considerable increase of attenuation from the BPF to the second harmonic, a

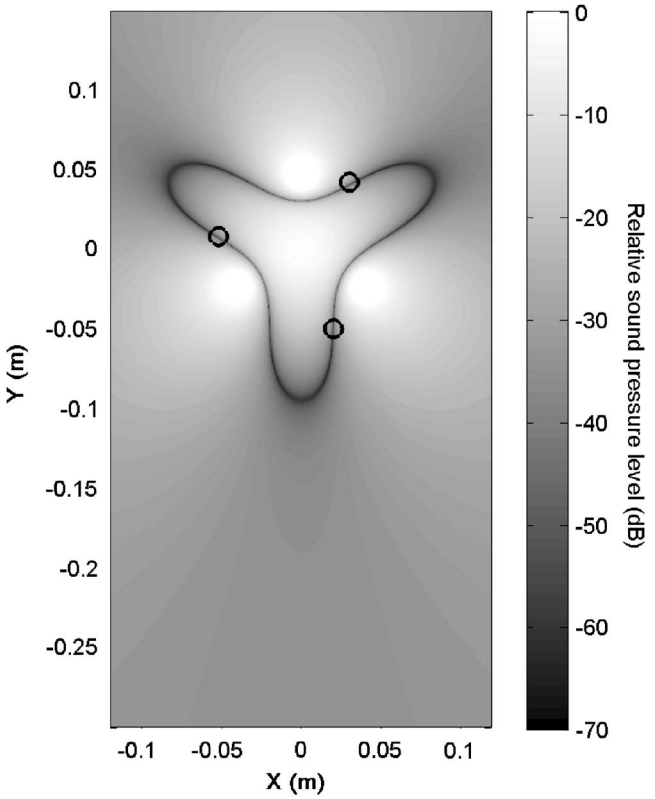


*Fig. 15—Theoretically predicted controlled acoustic pressure field of a plane containing a noise source and three control sources at* 600 Hz*, relative to the pressure field of a single monopole. The dark line indicates a pressure null demarcating optimal error sensor location on the plane, while the black markers indicate experimentally implemented locations.*

result that is not predicted by the theoretical model. An increase in frequency gives an increase in *kd*, which should decrease the possible attenuation by the control sources. A comparison to the minimum power radiation plot (Fig. 2) confirms that the BPF is not being attenuated as much as is ideally possible. The 600-Hz tone produces a *kd* value of 0.5, which predicts an attenuation of close to 35 dB in the ideal case.

*Table 1—Sound power reduction (in dB) achieved experimentally by three symmetrically-spaced control sources surrounding a* 60-mm *fan.*

| | Achieved SPR |
|---|---|
| BPF | 14.8 |
| 2 × BPF | 15.7 |
| 3 × BPF | 8.5 |

It was initially suspected that the smaller reduction might be attributed to poor actuator low-frequency response at 600 Hz. However, this hypothesis was ruled out—a total harmonic distortion analysis showed negligible harmonic distortion at the typical driving voltages of the control loudspeakers. Further investigation revealed that at the error sensor signal the control system had attenuated the BPF very close to the broadband noise level, as seen in Fig. 16. This suggests that the broadband noise floor at 600 Hz may have been limiting the control at that frequency. The noise attenuation at the error sensor at 600 Hz is seen to be nearly 25 dB. Because the theory suggests that this location should be a pressure null, it is not surprising that this value is greater than the attenuation actually achieved in the far field.

In the case of the second harmonic, the attenuation at 1200 Hz approached the predicted theoretical limit much more closely than the BPF. The experimental reduction was approximately 5 dB less than that predicted as ideal for the 60-mm control system. The SPL at 1200 Hz at the error sensor, however, is again seen in Fig. 16 to be at the noise floor, as in the 600-Hz case.

For the third harmonic, comparison of the achieved reduction to the theoretical limit shows that the attenuation at 1800 Hz is again close to 5 dB less than the theoretical power reduction. In this case, however, the 1800-Hz tone at the error sensor was not attenuated down to the noise floor as with the first two harmonics. This result indicates that the broadband noise floor is not the limiting factor in the global reductions achieved for the third harmonic. Rather, it is the sampling rate of the processor that is suspected. Snyder suggests that in order to achieve optimal active control, one should use a sampling rate that is at least 10 times the target frequency, but no more than 50 times the target frequency, though reasonable control has been shown with a sampling rate as low as three times the target frequency[13]. It is noted that in this case global control was exhibited at 1.8 kHz with a 4-kHz sampling frequency—a factor of 2.22. Despite the fact that control was achieved at 1.8 kHz, being so close to the Nyquist frequency may have adversely affected the control performance and explain the third harmonic not being attenuated to the noise floor, as were the first and second harmonics. While not yet achieving theoretical limits for possible sound power reduction, reduction of the second and third harmonics for the 60-mm control system appears to approach the predicted ideals.

### 5.2 60-mm System vs. 80-mm System

Perhaps the most significant difference between the current and previous control systems was the control of

*Table 2—Overall noise reduction comparison (in dB) of the* 60-mm *control system, the* 80-mm *control system, and the theoretically ideal sound power reduction. Experimental reductions of the two control systems are given in sound power level reduction (SPR).*

| | 60-mm fan | | | 80-mm fan | | |
|---|---|---|---|---|---|---|
| | *kd* | Predicted SPR | Achieved SPR | *kd* | Predicted SPR | Achieved SPR |
| BPF | 0.5 | 34.6 | 14.5 | 0.4 | 37.9 | 6.7 |
| 2×BPF | 1.0 | 21.9 | 16.6 | 0.8 | 25.4 | 16.5 |
| 3×BPF | 1.5 | 13.8 | 9.0 | 1.2 | 19.5 | 14.9 |

the BPF. The 60-mm control system achieved SPR nearly 8 dB greater than that achieved by the 80-mm control system, despite the fact that *kd* for the 60-mm fan was 25% greater. This is because the 80-mm system achieved significant far-field reductions on-axis (approximately 25 dB at some locations), but little control off-axis. A comparison of Figs. 8 and 12 shows that the global reduction of the 60-mm fan noise was much more uniform. The relatively poor control for the 80-mm system at BPF may have been partly due to a poor loudspeaker frequency response at 370 Hz for the control loudspeakers used in the 80-mm control system[7]. However, the reasons for the non-uniformity of the control at the BPF for the 80-mm fan are not well understood. The increase of frequency to 600 Hz appears to have positively affected control of the BPF, even though the actuator size was decreased. The loudspeakers used with the 60-mm system, while smaller, were also higher quality drivers with higher power-handling capabilities.

At their second harmonics, the two systems achieved nearly identical sound power reductions, approximately

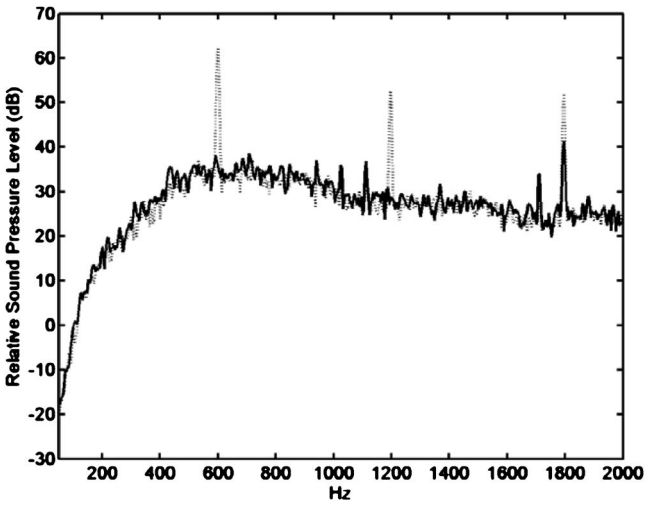


*Fig. 16—Typical measured error sensor spectrum for the* 60-mm *system with (solid) and without (dotted) active noise control.*

16.5 dB. This result indicates better performance of the 60-mm fan system, again because *kd* is 25% greater. However, it is worth noting that the limiting factor in both cases may be the broadband noise floors of the fans. The controller for the 80-mm fan reduced the second harmonic down to the broadband noise at the error sensor[14], and the controller for the 60-mm fan reduced the BPF and the second harmonic down to the broadband noise (see Fig. 16)

For the third harmonics, a difference in SPR of nearly 6 dB is seen, this time in favor of the 80-mm system. This may be attributed to the sampling frequency limitation discussed previously, where the third harmonic for the 60-mm fan approaches the Nyquist frequency of the controller. On the other hand, the third harmonic for the 80-mm fan is significantly lower in frequency (1110 Hz) and was able to be reduced to the broadband levels at the error sensor. This suggests that at 3×BPF, different constraints limit performance of the two control systems to approximately 5 dB less than the theoretical predictions. However, it is worth noting that the performance of the two systems at their respective third harmonics, in fact, follows the theoretical trend predicted by the analytical model. An increase in *kd* from 1.2 (80-mm) to 1.5 (60-mm) in Fig. 2 results in a reduction of maximum SPR of approximately 6 dB, which has been observed here experimentally.

## 6 CONCLUSIONS

The 60-mm fan control system exhibited similar control performance to that of the 80-mm fan control system developed by Gee and Sommerfeldt. Significant improvement was seen in the control performance of the BPF because of the control loudspeakers used, and perhaps because of stronger tonal components. This suggests that replacement of an 80-mm fan with the 60-mm fan and control system is a feasible step toward making active control a more practical method of reducing axial cooling fan noise. With the 60-mm fan and control actuator configuration meeting the spatial

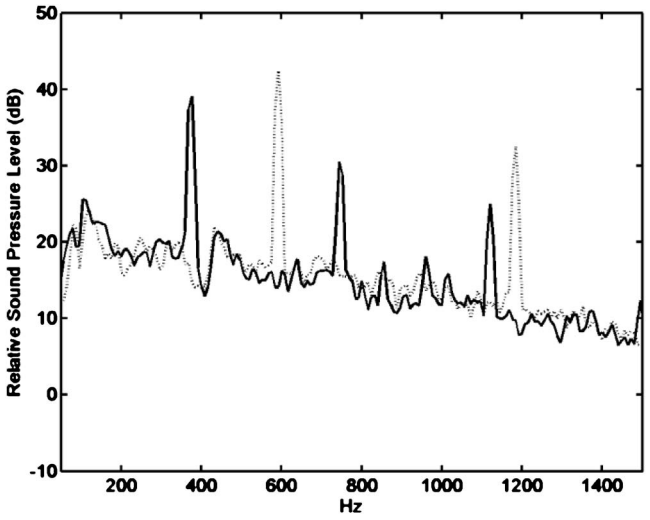


*Fig. 17—On-axis comparison at approximately one meter of* 80-mm *fan broadband spectrum (solid) and* 60-mm *fan broadband spectrum (dotted).*

constraint of an $80 \times 80$-mm$^2$ area, the need for manipulation of current electronic equipment design is minimal. It is also noteworthy that, although this would require modification to fan housing designs, three symmetrically oriented loudspeakers demonstrates nearly identical performance to the four-source system. This result is in line with theoretical predictions.

Although the experimentally achieved sound power reductions do not match theoretical ideals, the experimental work performed on the 60-mm control system appears to support the theoretical predictions of the four-control source geometry. The second and third harmonics, in particular, approach the predicted ideal attenuation. Discrepancies may be due to the broadband noise floor for lower harmonics and perhaps due to processor limitations for the highest harmonic controlled.

Additional work in the area of free-field fan noise control is anticipated. For this work, processor limitations constrained the maximum sampling frequency to 4 kHz. Employment of a faster processor would allow a greater sampling rate, and could thereby increase the range of frequencies that can be significantly controlled. Also, this research did not attempt to control the broadband component of the fan noise with ANC. Figure 17 shows an on-axis comparison of the 80-mm fan spectrum versus the 60-mm fan spectrum, indicating that the broadband noise levels are similar. If sufficient control is demonstrated on the tonal noise, the broadband noise will become dominant. Efforts are currently being made to globally reduce the broadband noise using ANC[15].

An additional consideration for practical implementation is the cost of the system. While an exact current cost is not available, indications are that the hardware cost could be less than 20 USD. Many fans now have a tach signal available that would eliminate the need for an emitter/detector pair to obtain a suitable reference input signal. In addition, as mentioned previously, the system has already been tested with inexpensive electret microphones and essentially identical control results were obtained. Finally, several possible inexpensive DSP solutions exist, such that several manufacturers feel the final cost may even be less than 10 USD. Further work is also focusing on resolving these remaining issues.

## 7 REFERENCES


1. G. W. Evans and D. Johnson, "Stress and open-office noise," *J. Appl. Psychol.* **85**, 779–783, (2000).
2. K. D. Kryter and K. S. Pearsons, "Judged Noisiness of a Band of Random Noise Containing an Audible Pure Tone," *J. Acoust. Soc. Am.* **38**, 106–112, (1965).
3. D. A. Quinlan, "Application of active control to axial flow fans," *Noise Control Eng. J.* **39**, 95–101, (1992).
4. M. Q. Wu, "Active cancellation of small cooling fan noise from office equipment," *Proc. INTER-NOISE 95*, edited by Robert J. Bernhard and J. Stuart Bolton, Vol. 2, pp. 525–528, (1995).
5. G. C. Lauchle, J. R. MacGillivray and D. C. Swanson, "Active control of axial-flow fan noise," *J. Acoust. Soc. Am.* **101**, 341–349, (1997).
6. K. Homma, C. Fuller and K. X. Man, "Broadband Active-Passive Control of Small Axial Fan Noise Emission," *Proc. NOISE-CON 2003*, (2003).
7. K. L. Gee and S. D. Sommerfeldt, "A compact active control implementation for axial cooling fan noise," *Noise Control Eng. J.* **51**(6), 325–334, (2003).
8. S. D. Sommerfeldt, "Multi-channel adaptive control of structural vibration," *Noise Control Eng. J.* **37**, 77–89, (1991).
9. K. L. Gee and S. D. Sommerfeldt, "Application of theoretical modeling to multichannel active control of cooling fan noise," *J. Acoust. Soc. Am.* **115**, 228–236, (2004).
10. P. A. Nelson and S. J. Elliott, *Active Control of Sound*, Academic, London, (1992).
11. C. H. Hansen and S. D. Snyder, *Active Control of Noise and Vibration*, E&FN Spon, London, (1997).
12. T. W. Leishman, S. Rollins and H. M. Smith, "An experimental evaluation of regular polyhedron loudspeakers as omnidirectional sources of sound," *J. Acoust. Soc. Am.* **120**, 1411–1422, (2006).
13. S. D. Snyder, "Microprocessors for active control: Bigger is not always enough," *Proc. Active 99*, 45–62, (1999).
14. K. L. Gee, "Multi-channel active control of axial cooling fan noise," MS Thesis, Brigham Young University, Provo Utah, (2002).
15. M. Green, S. D. Sommerfeldt and B. M. Faber, "Feedback control of broadband axial fan noise for global attenuation," *Proc. Active 2006*, (2006).